Thin-film InAs/GaAs quantum dot solar cell with planar and pyramidal back reflectors

Thin-film InAs/GaAs quantum dot solar cell with planar and pyramidal back reflectors

TIMO AHO,[1,*] FARID ELSEHRAWY,[2] ANTTI TUKIAINEN,[1] SANNA RANTA,[1] MARIANNA RAAPPANA,[1] RIKU ISOAHO,[1] ARTO AHO,[1] ARTTU HIETALAHTI,[1] FEDERICA CAPPELLUTI,[2] AND MIRCEA GUINA [1]

[1] *Optoelectronics Research Centre, Physics Unit, Tampere University, 33720 Tampere, Finland*
[2] *Department of Electronics and Telecommunications, Politecnico di Torino, 10129 Torino, Italy*
**Corresponding author: timo.aho@tuni.fi*

Received XX Month XXXX; revised XX Month, XXXX; accepted XX Month XXXX; posted XX Month XXXX (Doc. ID XXXXX); published XX Month XXXX

Quantum dot solar cells are promising for next generation photovoltaics owing to their potential for improved device efficiency related to bandgap tailoring and quantum confinement of charge carriers. Yet implementing effective photon management to increase the absorptivity of the quantum dots is instrumental. To this end, the performance of thin-film InAs/GaAs quantum dot solar cells with planar and structured back reflectors is reported. The experimental thin-film solar cells with planar reflector exhibited a bandgap-voltage offset of 0.3 V with an open circuit voltage of 0.884 V, which is one of the highest values reported for quantum dot solar cells grown by molecular beam epitaxy. Using measured external quantum efficiency and current-voltage characteristics, we parametrize a simulation model that was used to design an advanced reflector with diffractive pyramidal gratings revealing a 12-fold increase of the photocurrent generation in the quantum dot layers.

http://dx.doi.org/10.1364/AO.99.099999

1. INTRODUCTION

Quantum dots (QDs) have gained interest for photovoltaics due to their ability to enhance the infrared spectral response of single-junction solar cells (SCs) thus increasing their short-circuit current densities (J_{sc}) [1, 2]. They also bring more options for tuning the bandgap in III–V multijunction SCs [3, 4] and have triggered the development of intermediate band SCs [5]. However, research in recent years has pinpointed several issues to solve for attaining the theoretical efficiency. These are largely linked to the relatively modest absorption provided by the QDs [6]. To enhance the absorption, a high number of QD layers and high QD densities are required [7], yet the fabrication of such structures with high crystalline quality is challenging. Moreover, with a high number of QD layers (>20 layers) the open-circuit voltage (V_{oc}) tends to decrease, in part due to the strain induced defects that compromise the material quality, and in part inherently related to the narrower bandgap of the quantum dots [2, 6, 8]. On the other hand, when using just a few QD layers (~10 layers), the V_{oc} degradation is marginal [9, 10] but the current enhancement is modest. To alleviate this limitation, a reflector can be applied on the back of the SC to increase the absorption length and the photocurrent. Implementing reflectors requires a thin-film architecture employing substrate removal, which brings additional benefits, in particular for applications where flexibility and high power-to-weight ratio are needed [11–13]. Thin-film QDSCs have been reported with planar back reflector [14, 15] and more recently with textured back reflector [16]. Furthermore, many structural concepts have been successfully introduced to solar cells enabling the light-trapping effect and increasing the photocurrent generation [17–22].

Here, we demonstrate the performance of a thin-film InAs/GaAs QDSC with a planar back reflector and compare it to the performance of a standard wafer-based (i.e., thick) QDSC. The enhancement in the QD photocurrent and the performance of the thin-film QDSC are benchmarked against those of the wafer based QDSC, using external quantum efficiency (EQE) and current-voltage (*I-V*) characteristics measured at different concentration. Based on the experimental data a simulation model is parametrized and used to design a diffractive back reflector employing pyramidal gratings to further enhance the photocurrent.

2. METHODS

A. Device concept

The QDSC structures studied are schematically presented in Fig. 1, all incorporating similar QD stacks. Two structures were experimentally fabricated: they are a standard wafer-based structure and thin-film (substrate removed) structure with a planar back reflector. A third structure, representing a thin-film architecture with a back reflector

incorporating pyramidal gratings was simulated based on experimental results obtained for the fabricated devices.

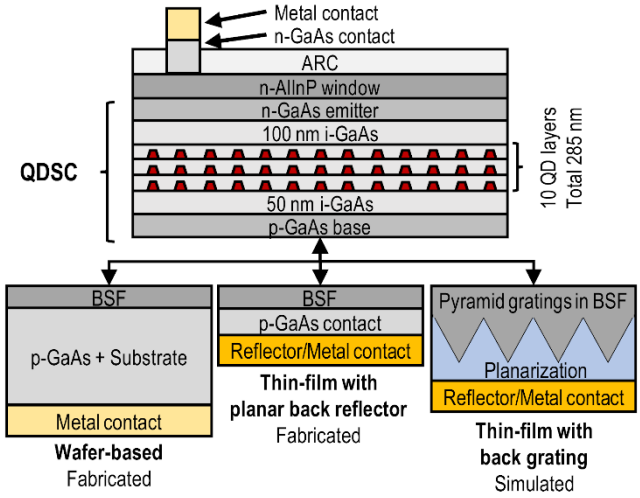

Fig. 1. Schematic drawings of the QDSCs: the wafer-based substrate configuration (left), the thin-film configuration with a planar back-side reflector (middle), and the simulated thin-film configuration with a back grating and a reflector (right).

B. Fabrication and characterization

The InAs/GaAs QDSCs were grown by molecular beam epitaxy (MBE) employing a shallow junction design with an *n*-doped emitter and a *p*-doped base [23]. The QDSC stack included 10 QD layers with an in-plane QD density of approximately 6×10^{10} 1/cm^2 separated by ~30 nm thick GaAs layers. The total thickness of the photogeneration layer in thin-film configuration is 0.75 µm. Such a thin layer is far from being optimum for terrestrial operation but was chosen in view of optimizing the cell performance after irradiation exposure [24]. The thin-film prototype included a thick AlInP window layer (600 nm) to enable the fabrication of nanostructured antireflection coating [25, 26]. The wafer-based structure is very similar with some minor differences that do not impact the analysis in this paper. The wafer-based QDSC was processed by leaving the substrate intact. Front Ni/Au and back Ti/Au contacts were deposited by electron beam (e-beam) evaporation using shadow mask. A TiO_2/SiO_2 antireflection coating (ARC) was deposited by e-beam evaporation in the areas where contact GaAs layer was removed by selective wet etching.

The thin-film QDSC was processed using the following steps. First, the planar Au reflector was deposited by e-beam evaporation on top of the *p*-GaAs contact layer of the inverted-grown structure. Pt and Au layers were evaporated on top of the reflector to act as a diffusion barrier and bonding contact layer, respectively. Subsequent to the metal deposition, the QDSC was indium bonded to a sub-mount. The substrate of the QDSC was thinned and polished to thickness of ~100 µm with a Logitech PM5 precision lapping machine. The rest of the substrate was removed by wet etching. Next, a front contact of Ni/Au was deposited on top of the *n*-GaAs contact layer by e-beam evaporation using a photolithographic lift-off process. The cells were electrically isolated by wet etching. Finally, the *n*-GaAs contact layer was wet etched and a TiO_2/SiO_2 ARC was deposited by e-beam evaporation.

For EQE measurements we used a 250 W quartz tungsten halogen lamp and a Digikrom DK240 monochromator equipped with an 800 nm long-pass filter. The signals were measured using an SRS SR830 lock-in amplifier and chopped light. A NIST-calibrated Ge reference detector was used as a reference. *I-V* characteristics were measured at 25 °C with a commercial OAI solar simulator using AM1.5D spectrum.

C. Modelling

The samples were designed using in-house numerical tools developed for QDSCs [27] and already validated against several experimental case studies [2, 28–30]. In this framework, electrical transport was modeled by a quantum-corrected drift-diffusion approach [27] coupled with a full wave electromagnetic model for optical generation. In particular, 3D rigorous coupled wave analysis was used for the case study with pyramid gratings [29, 31]. Optical properties of the bulk materials were taken from the literature for GaAs [32], AlInP and GaInP [33], and Ag [34]. Concerning QDs, the optical model assumes a three-level absorber with Lorentzian-shaped absorption bands corresponding to the wetting layer, excited state, and ground state. Full width at half maximum is about 50 nm and peak wavelengths are 920 nm, 1000 nm, and 1050 nm, as derived from the experimental photoluminescence spectra of the samples with uncapped QD layers. We assume typical absorption peak values of 2×10^4 1/cm, 1000 1/cm, and 500 1/cm for wetting layer, excited state, and ground state, respectively.

3. RESULTS AND DISCUSSIONS

The EQE spectra presented in Fig. 2(a) reveal the QD response in the wavelength range of 900–1100 nm. The QDSC with back reflector showed increased EQE when compared to the wafer-based QDSC.

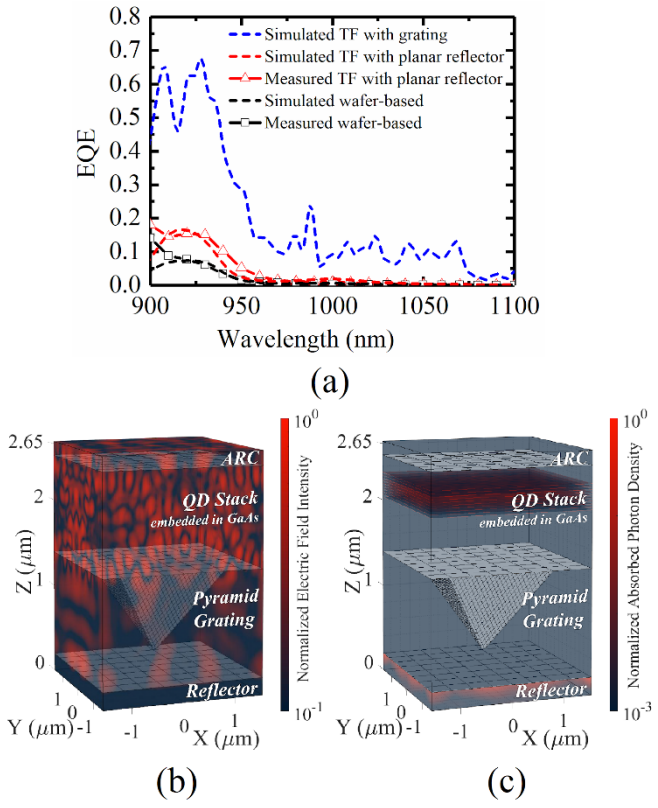

Fig. 2. (a) Measured and simulated EQE of the studied QDSCs. (b) Normalized electric field intensity and (c) absorbed photon density for the QDSC with pyramid back-side grating and reflector at λ = 1050 nm.

Experimental and simulated results are in good agreement, with some deviation near 900 nm, where the measured EQEs show higher values than the simulated ones. This could be related to the fabrication process

of the QDs, which induces an absorption band tail in the range between the GaAs band-edge and the QD wetting layer states [35], whereas simulations assume a GaAs absorption profile with a sharp cut-off at 870 nm. The calculation of J_{sc} by integrating the measured (simulated) EQE over the AM1.5D solar spectrum (1000 W/m²) in the wavelength range of 900–1100 nm yields a J_{sc} of 0.17 (0.16) mA/cm² and 0.35 (0.33) mA/cm² for the wafer-based QDSC and the QDSC with the back reflector, respectively. Thus, the QDSC with the back reflector enhances approximately twice the current of the QDSC.

The I-V results of the thin-film QDSC with the planar back reflector are presented in Fig. 3, and Table 1 summarizes the measured and simulated photovoltaic figures of merit. Simulations provide a target value since they neglect any extrinsic recombination mechanism. We see a good match in terms of J_{sc}, indicating that at short-circuit condition, photogenerated carrier loss is negligible for the fabricated samples. The fill factor (FF) of the thin-film solar cell is markedly lower than the theoretical value but also lower than the value (80%) found for the wafer-based sample. Presumably, the difference between the thin-film and wafer-based cells results from the fact that in the thin-film SC, the Au back reflector (also the electrical contact) is not forming an ohmic contact with the p-GaAs contact layer, due to the not sufficiently high doping level. Based on our previous study [36], the Au reflector should form an ohmic contact if the doping level of the *p*-GaAs layer is high enough. For the wafer-based QDSC, the ohmic contact is formed between the highly doped *p*-GaAs wafer and the back metal.

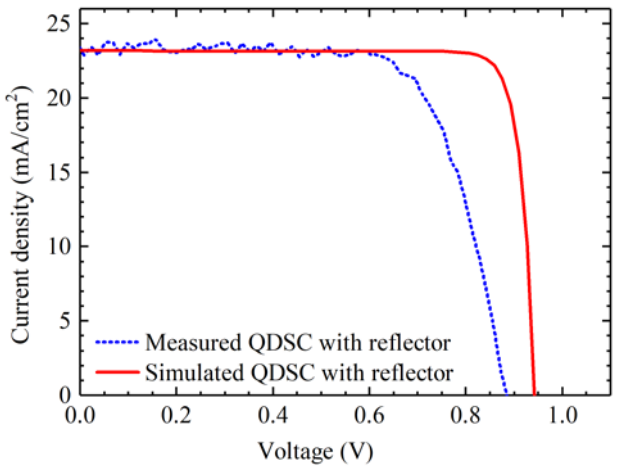

Fig. 3. Measured and simulated *I-V* results of the thin-film QDSC with planar back reflector at one sun AM1.5D (1000 W/m²).

Table 1. Measured and simulated *I-V* results of the thin-film QDSC with planar back reflector at one sun AM1.5D (1000 W/m²).

	J_{sc}	V_{oc}	FF	Efficiency
	(mA/cm²)	(V)	(%)	(%)
Measured	23.4	0.884	71	14.7
Simulated	23.2	0.942	87	19.1

The experimental V_{oc} of 0.884 V exhibited by the QDSC with the back reflector is high when compared to the reported values for other QDSCs [2, 14, 37], but is about 60 mV lower than the designed value. The simulated V_{oc} implies a bandgap-voltage offset of about 0.24 V (measured 0.3 V) with respect to the QD ground state energy (1.18 eV), which can be understood as the consequence of radiative recombination through the QDs. To grasp the cause of the extra 60 mV loss, *I-V* measurements were carried out at varying concentrations for both the wafer-based and thin-film samples. As shown in Fig. 4, J_{sc} scales almost linearly with the concentration factor (C), confirming that the samples are operating as a conventional single-junction cell (in contrast, in intermediate band operation J_{sc} scales super-linearly with the concentration factor [14]). Expressing the current density as J_{sc} (C) = C $J_{sc}^{1\ sun}$, and using the diode equation, the dependence of V_{oc} on concentration is given as Eq. (1):

$$V_{oc}\ (\mathrm{C}) = V_{oc}^{1\ sun} + \eta V_T \ln(\mathrm{C}), \qquad \textbf{(1)}$$

where η being the diode ideality factor. From Fig. 4, the extracted value of η is about 1.4 for both solar cells. This suggests that the dark current has an extrinsic component, due to nonradiative recombination in the intrinsic layer stack, which causes the 60 mV penalty with respect to the designed value. Such penalty is similar in the wafer-based and thin-film samples, demonstrating that the V_{oc} is otherwise preserved during the thin-film processing, while there is still some margin of improvement in terms of epitaxial growth.

With the validated physical model based on planar reflector experiment, we simulated the performance of a thin-film QDSC that utilizes a back reflector with pyramid gratings fabricated into an AlInP back surface field (BSF) layer and planarized with a polymer layer (Fig. 1). In this case, light is diffracted from the back reflector, resulting in multiple passes through the photoactive layer. A preliminary experimental and simulation study on textured polymer/metal reflectors indicated that the pyramidal patterning is the most promising one in terms of diffraction efficiency [29]. The calculated EQE spectrum shown in Fig. 2(a) demonstrates a remarkable increase of the cell absorbance in the textured thin-film sample. The excitation of high diffraction orders is well visible in the distribution of the electric field intensity (at the wavelength of 1050 nm) reported in Fig. 2(b). This provides a genuine enhancement of the absorbed photon density in the QD stack, as shown in Fig. 2(c), with some residual yet marginal loss in the metal reflector.

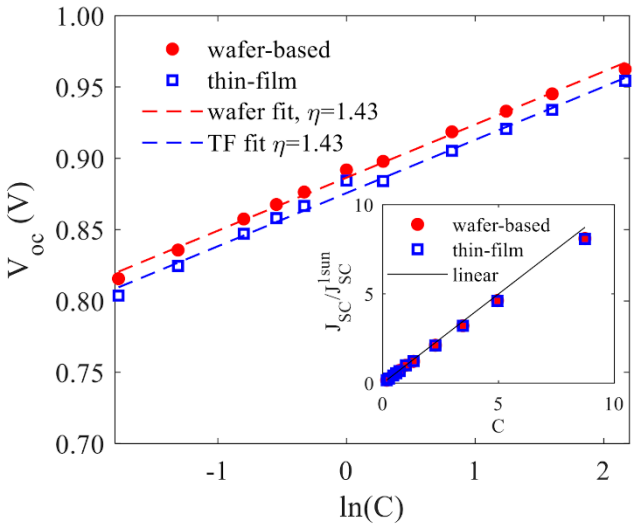

Fig. 4. V_{oc} as a function of the concentration factor. In the inset, short-circuit current density J_{sc} normalized by the J_{sc} at 1 sun illumination.

As a result, the QD photocurrent density rises to 1.89 mA/cm², i.e., the cell incorporating the pyramidal grating works as equivalent to a virtual stack with 12 times the number of QD layers or QD areal density. Such

improvement is instrumental to achieve high-efficiency QDSCs, since it enhances the cell absorptivity without increasing thermalization losses.

4. CONCLUSIONS

The impact of back reflectors on the performance of MBE-grown thin-film InAs/GaAs QDSCs was assessed. The photocurrent generation in the QD layers is increased by a factor of two when the thin-film configuration utilizing a planar back reflector is compared to the wafer-based QDSC while the performance in terms of V_{oc} is preserved. Based on the simulations, a 12-fold increase of photocurrent generation in the QD layers could be achieved by employing diffractive gratings on the backside of the QDSC. The QDSC with back reflector exhibited a bandgap-voltage offset of about 0.3 V with respect to the QD ground state energy, mostly due to radiative recombination through the QDs. The demonstrated V_{oc} of 0.884 V is one of the highest V_{oc} values reported for MBE-grown QDSCs.

Funding. European Union, Horizon 2020 project TFQD (Grant Agreement No. 687253). European Union, ERC AdG project AMETIST (Grant Agreement No. ERC-2015-AdG 695116). Academy of Finland, Flagship Programme PREIN #320168.

Acknowledgments. The author acknowledges Jenny and Antti Wihuri Foundation for their support and would like to thank Ville Polojärvi and Elina Anttola for their technical support.

Disclosures. The authors declare no conflicts of interest.

REFERENCES

1. V. Aroutiounian, S. Petrosyan, A. Khachatryan, and K. Touryan, "Quantum dot solar cells," J. Appl. Phys. **89**(4), 2268-2271 (2001).
2. F. Cappelluti, M. van Eerden, A. P. Cédola, T. Aho, G. Bissels, F. Elsehrawy, J. Wu, H. Liu, P. Mulder, G. J. Bauhuis, J. J. Schermer, T. Niemi, and M. Guina, "Light-trapping enhanced thin-film III-V quantum dot solar cells fabricated by epitaxial lift-off," Sol. Energy Mater. Sol. Cells **181**, 83-92 (2018).
3. W. Ho, Y. Lee, G. Yang, and C. Chang, "Optical and electrical characteristics of high-efficiency InGaP/InGaAs/Ge triple-junction solar cell incorporated with InGaAs/GaAs QD layers in the middle cell," Prog. Photovolt: Res. Appl. **24**(4), 551-559 (2016).
4. C. Kerestes, S. Polly, D. Forbes, C. Bailey, A. Podell, J. Spann, P. Patel, B. Richards, P. Sharps, and S. Hubbard, "Fabrication and analysis of multijunction solar cells with a quantum dot (In)GaAs junction," Prog. Photovolt: Res. Appl. **22**(11), 1172-1179 (2014).
5. A. Luque and A. Martí, "Increasing the efficiency of ideal solar cells by photon induced transitions at intermediate levels," Phys. Rev. Lett. **78**(26), 5014 (1997).
6. A. Mellor, A. Luque, I. Tobías, and A. Martí, "The feasibility of high-efficiency InAs/GaAs quantum dot intermediate band solar cells," Sol. Energy Mater. Sol. Cells **130**, 225-233 (2014).
7. K. Sakamoto, Y. Kondo, K. Uchida, and K. Yamaguchi, "Quantum-dot density dependence of power conversion efficiency of intermediate-band solar cells," J.Appl.Phys. **112**(12), 124515 (2012).
8. T. Sugaya, O. Numakami, R. Oshima, S. Furue, H. Komaki, T. Amano, K. Matsubara, Y. Okano, and S. Niki, "Ultra-high stacks of InGaAs/GaAs quantum dots for high efficiency solar cells," Energy Environ. Sci. **5**(3), 6233-6237 (2012).
9. D. Guimard, R. Morihara, D. Bordel, K. Tanabe, Y. Wakayama, M. Nishioka, and Y. Arakawa, "Fabrication of InAs/GaAs quantum dot solar cells with enhanced photocurrent and without degradation of open circuit voltage," Appl. Phys. Lett. **96**(20), 203507 (2010).
10. C. G. Bailey, D. V. Forbes, S. J. Polly, Z. S. Bittner, Y. Dai, C. Mackos, R. P. Raffaelle, and S. M. Hubbard, "Open-circuit voltage improvement of InAs/GaAs quantum-dot solar cells using reduced InAs coverage," IEEE J. Photovolt. **2**(3), 269-275 (2012).
11. F. Cappelluti, G. Ghione, M. Gioannini, G. Bauhuis, P. Mulder, J. Schermer, M. Cimino, G. Gervasio, G. Bissels, and E. Katsia, "Novel concepts for high-efficiency lightweight space solar cells," in Proceedings of 11th European Space Power Conference, (EDP Sciences, 2017), pp. 03007.
12. N. Baldock and M. R. Mokhtarzadeh-Dehghan, "A study of solar-powered, high-altitude unmanned aerial vehicles," Aircraft Eng. Aerospace Technol. **78**(3), 187-193 (2006).
13. R. Tatavarti, G. Hillier, A. Dzankovic, G. Martin, F. Tuminello, R. Navaratnarajah, G. Du, D. P. Vu, and N. Pan, "Lightweight, low cost GaAs solar cells on 4" epitaxial liftoff (ELO) wafers," in Proceedings of IEEE 33rd Photovoltaic Specialists Conference (PVSC), (IEEE, 2008), pp. 1-4.
14. T. Sogabe, Y. Shoji, P. Mulder, J. Schermer, E. Tamayo, and Y. Okada, "Enhancement of current collection in epitaxial lift-off InAs/GaAs quantum dot thin film solar cell and concentrated photovoltaic study," Appl. Phys. Lett. **105**(11), 113904 (2014).
15. M. F. Bennett, Z. S. Bittner, D. V. Forbes, S. Rao Tatavarti, S. Phillip Ahrenkiel, A. Wibowo, N. Pan, K. Chern, and S. M. Hubbard, "Epitaxial lift-off of quantum dot enhanced GaAs single junction solar cells," Appl. Phys. Lett. **103**(21), 213902 (2013).
16. B. L. Smith, M. A. Slocum, Z. S. Bittner, Y. Dai, G. T. Nelson, S. D. Hellstroem, R. Tatavarti, and S. M. Hubbard, "Inverted growth evaluation for epitaxial lift off (ELO) quantum dot solar cell and enhanced absorption by back surface texturing," in Proceedings of IEEE 43rd Photovoltaic Specialists Conference (PVSC), (IEEE, 2016), pp. 1276-1281.
17. S. Mokkapati and K. R. Catchpole, "Nanophotonic light trapping in solar cells," J. Appl. Phys. **112**(10), 101101 (2012).
18. M. L. Brongersma, Y. Cui, and S. Fan, "Light management for photovoltaics using high-index nanostructures," Nature materials **13**(5), 451-460 (2014).
19. H. Chen, A. Cattoni, R. De Lépinau, A. W. Walker, O. Höhn, D. Lackner, G. Siefer, M. Faustini, N. Vandamme, and J. Goffard, "A 19.9%-efficient ultrathin solar cell based on a 205-nm-thick GaAs absorber and a silver nanostructured back mirror," Nature Energy **4**(9), 761-767 (2019).
20. W. Cao, J. D. Myers, Y. Zheng, W. T. Hammond, E. Wrzesniewski, and J. Xue, "Enhancing light harvesting in organic solar cells with pyramidal rear reflectors," Appl. Phys. Lett. **99**(2), 135 (2011).
21. M. I. Hossain, W. Qarony, M. K. Hossain, M. K. Debnath, M. J. Uddin, and Y. H. Tsang, "Effect of back reflectors on photon absorption in thin-film amorphous silicon solar cells," Applied Nanoscience **7**(7), 489-497 (2017).
22. M. M. Tavakoli, H. T. Dastjerdi, J. Zhao, K. E. Shulenberger, C. Carbonera, R. Po, A. Cominetti, G. Bianchi, N. D. Klein, and M. G. Bawendi, "Light management in organic photovoltaics processed in ambient conditions using ZnO nanowire and antireflection layer with nanocone array," Small **15**(25), 1900508 (2019).
23. A. Tukiainen, J. Lyytikäinen, T. Aho, E. Halonen, M. Raappana, F. Cappelluti, and M. Guina, "Comparison of 'shallow'and 'deep'junction architectures for MBE-grown InAs/GaAs quantum dot solar cells," in Proceedings of IEEE 7th World Conference on Photovoltaic Energy Conversion (WCPEC), (IEEE, 2018), pp. 2950-2952.
24. L. C. Hirst, M. K. Yakes, J. H. Warner, M. F. Bennett, K. J. Schmieder, R. J. Walters, and P. P. Jenkins, "Intrinsic radiation tolerance of ultra-thin GaAs solar cells," Appl. Phys. Lett. **109**(3), 033908 (2016).
25. J. Tommila, V. Polojärvi, A. Aho, A. Tukiainen, J. Viheriälä, J. Salmi, A. Schramm, J. M. Kontio, A. Turtiainen, and T. Niemi, "Nanostructured broadband antireflection coatings on AlInP fabricated by nanoimprint lithography," Sol. Energy Mater. Sol. Cells **94**(10), 1845-1848 (2010).
26. F. Elsehrawy, T. Aho, T. Niemi, M. Guina, and F. Cappelluti, "Improved Light Trapping in Quantum Dot Solar Cells Using Double-sided

Nanostructuring," in Proceedings of Optics and Photonics for Energy and the Environment, (Optical Society of America, 2018), pp. JM4A. 5.
27. M. Gioannini, A. P. Cedola, N. Di Santo, F. Bertazzi, and F. Cappelluti, "Simulation of quantum dot solar cells including carrier intersubband dynamics and transport," IEEE J. Photovolt. **3**(4), 1271-1278 (2013).
28. A. P. Cédola, D. Kim, A. Tibaldi, M. Tang, A. Khalili, J. Wu, H. Liu, and F. Cappelluti, "Physics-based modeling and experimental study of si-doped inas/gaas quantum dot solar cells," Int. J. Photoenergy **2018**, 7215843 (2018).
29. T. Aho, M. Guina, F. Elsehrawy, F. Cappelluti, M. Raappana, A. Tukiainen, A. K. Alam, I. Vartiainen, M. Kuittinen, and T. Niemi, "Comparison of metal/polymer back reflectors with half-sphere, blazed, and pyramid gratings for light trapping in III-V solar cells," Opt. Express **26**(6), A331-A340 (2018).
30. A. Khalili, A. Tibaldi, F. Elsehrawy, and F. Cappelluti, "Multiscale device simulation of quantum dot solar cells," in Proceedings of Physics, Simulation, and Photonic Engineering of Photovoltaic Devices VIII, (International Society for Optics and Photonics, 2019), pp. 109131N.
31. F. Elsehrawy, A. Tibaldi, and F. Cappelluti, "Efficient multiphysics modeling of thin-film solar cells with periodically textured surfaces," in Proceedings of Physics, Simulation, and Photonic Engineering of Photovoltaic Devices VIII, (International Society for Optics and Photonics, 2019), pp. 109130K.
32. E. D. Palik, *Handbook of optical constants of solids* (Academic press, 1998).
33. "Sopra database," http://sspectra.com/sopra.html.
34. A. D. Rakić, A. B. Djurišić, J. M. Elazar, and M. L. Majewski, "Optical properties of metallic films for vertical-cavity optoelectronic devices," Appl. Opt. **37**(22), 5271-5283 (1998).
35. T. Li and M. Dagenais, "Below-bandgap absorption in InAs/GaAs self-assembled quantum dot solar cells," Prog. Photovolt: Res. Appl. **23**(8), 997-1002 (2015).
36. T. Aho, A. Aho, A. Tukiainen, V. Polojärvi, T. Salminen, M. Raappana, and M. Guina, "Enhancement of photocurrent in GaInNAs solar cells using Ag/Cu double-layer back reflector," Appl. Phys. Lett. **109**(25), 251104 (2016).
37. Y. Shoji, K. Watanabe, and Y. Okada, "Photoabsorption improvement in multi-stacked InGaAs/GaAs quantum dot solar cell with a light scattering rear texture," Sol. Energy Mater. Sol. Cells **204**, 110216 (2020).